FLUCTUATIONS AND NOISE IN KINETIC SYSTEMS

APPLICATION TO K^+ CHANNELS IN THE SQUID AXON

YI-DER CHEN *and* TERRELL L. HILL

From the Laboratory of Molecular Biology, National Institute of Arthritis, Metabolism, and Digestive Diseases, National Institutes of Health, Bethesda, Maryland 20014

ABSTRACT We consider the equilibrium or steady-state noise power density spectrum in the quantity $N = \sum_{i=0}^{x} a_i N_i$ for an ensemble of independent and equivalent systems each of which can exist in the discrete set of states $i = 0, 1, \cdots, x$. N_i is the number of systems of the ensemble in state i and the a_i's are constants. There is a transition rate constant α_{ij} for an arbitrary transition $i \to j$; the kinetic equations are linear. There are possible applications to enzyme and biochemical kinetics generally, to membrane transport, muscle contraction, binding on macromolecules, etc. In each case, noise measurements would provide information about the kinetic scheme. The particular application considered here is to K^+ channels or gates (one channel = one system) in the squid axon membrane: $a_i g_K$ is the K^+ conductance of a channel in state i and the kinetic scheme is of the Hodgkin-Huxley type (HH). Here we allow an arbitrary set of a_i's. This is a generalization of our treatment of K^+ channel noise in an earlier paper. The theory is discussed and some calculations made using Fishman's recent experimental results on K^+ channel noise as a guide. Preliminary indications are that the HH choice of a_i's may be oversimplified and that $a_0 \cong 0$, $a_1 \neq a_0$, $a_x \neq a_{x-1}$. Quite possibly the a_i's increase from a_0 to a_x, though the early a_i's must be relatively small to give the observed induction behavior in $g_K(t)$. An increase in equal steps is unsatisfactory because this is essentially HH with $x = 1$ (no induction). More refined experiments may modify these tentative conclusions. In any case, it appears from Fishman's work that noise measurements will probably be very useful in distinguishing between rival models of K^+ channels.

1. INTRODUCTION

The present work is an extension of an earlier paper (1) on noise in K^+ channels of the squid axon membrane. We assume familiarity with the notation and general approach of reference 1.

Since noise involves the decay of spontaneous fluctuations, noise measurements provide information about the governing kinetic scheme. Although our original

motivation arose from the K^+ channel problem, the analysis in this paper also applies to noise in many other equilibrium and steady-state systems: enzyme and biochemical kinetics, membrane transport and binding, steady-state cycling of cross-bridges in muscle, binding of ligands on biopolymers, etc. The only requirement is that we have an ensemble of independent and equivalent systems, each of which can be represented by a linear kinetic scheme or diagram as described below. The fluctuating quantity need not be electrical in nature; if it is not, an appropriate transducer can be used to convert it into an electrical signal.

At the time of its writing, the theoretical results in reference 1 seemed negative in the sense that the Hodgkin-Huxley (2) model (HH), and several variations of it, yielded $G(f)$'s which behaved more or less like $(1 + 4\pi^2 f^2 \tau^2)^{-1}$, whereas experiments indicated $G \sim 1/f$. Here $G(f)$ is the power density spectrum of fluctuations in the steady-state K^+ current, f is the frequency, and τ is the HH time constant for the open-close of K^+ channels. But this qualitative discrepancy appears to have been resolved in recent experiments reported by Fishman (3). By use of tetraethylammonium ion (TEA), which is known to block K^+ channels, Fishman was able to subtract a residual (i.e. with TEA present) $1/f$ noise component from the total spectrum (no TEA) to obtain a difference spectrum which is qualitatively of the form $(1 + 4\pi^2 f^2 \tau^2)^{-1}$, with a time constant of the order of the HH τ. Therefore, it now appears that the $1/f$ component is associated with modes of K^+ membrane transport other than via K^+ channels, while the remainder of the noise (the "difference spectrum") is related to the open-close of K^+ channels. Noise arising from steady-state K^+ current through an already open channel is presumably higher frequency noise (1) than that of interest here.

Thus the open-close kinetics of K^+ channels can now be related to steady-state noise (3) as well as to the classical voltage clamp K^+ current $I_K(t)$ (reference 2). After the experimental techniques are refined further (3), noise measurements will provide a new and probably more sensitive test of channel open-close models. For this reason we have thought it worthwhile to extend our treatment of K^+ noise in reference 1 to a rather more general class of models.

Section 2 contains a mathematical derivation of relevant noise properties for the class of models considered. In section 3 we comment on certain related aspects of the papers by Fishman (3), Stevens (4), and Lax (5). Section 4 presents a few illustrative numerical results, based on section 2, which are pertinent to Fishman's paper (3).

2. THE MODEL AND ITS NOISE SPECTRUM

We begin with a rather general model and then specialize in two steps which will be indicated by subsection headings. In all three parts of this section, the results should apply to a number of systems other than nerve membrane channels.

We consider an ensemble of M independent and equivalent systems (one system

equals one K^+ channel or gate in the case of primary interest) each of which can exist in the discrete set of states 0, 1, 2, $\cdots$, x. The transition probability, or rate constant, between any two states $i \rightarrow j$ is α_{ij}. (Note that transitions are not limited here to $i \rightarrow i + 1$ and $i \rightarrow i - 1$.) The α_{ij} are constants in any given steady-state noise calculation and have values such that the ensemble reaches equilibrium or a stationary steady state at $t = \infty$. The mean number of systems in state i is $\bar{N}_i$ and the probability that a system is in state i is $p_i = \bar{N}_i/M$. We shall indicate $t = \infty$ values by $\bar{N}_i^e$ and p_i^e and initial values by $N_i(0)$ and $p_i^0 = N_i(0)/M$. The master equation and some properties of the approach of the ensemble to steady state have been discussed elsewhere (6, 7). A diagram method (8) is useful, in complicated cases, in calculating the p_i^e from the α_{ij}.

Our primary objective is to find the power density spectrum $G(f)$ of fluctuations in the quantity N^e, where

$$N \equiv \sum_{i=0}^{x} a_i N_i, \tag{1}$$

and the a_i's are a set of positive constants. For convenience, the states 0, 1, $\cdots$, x are labeled in increasing order of the a_i's, with the largest, a_x, assigned the value $a_x \equiv 1$.

In the K^+ membrane current case, the physical significance of N is the following. The mean steady-state K^+ current carried by M channels is

$$\bar{I}_K^e = \bar{g}_K \bar{N}^e (V - E_K). \tag{2}$$

That is, the conductance of one channel in state i is $\bar{g}_K a_i$ ($\bar{g}_K$, as in HH notation, is the conductance in state x). We assume here (1) that fluctuations in I_K^e on a millisecond time scale arise from fluctuations in the equilibrium numbers N_i^e of channels in the various states. These fluctuations are, of course, due to interstate transitions (governed by the α_{ij}). Fluctuations in $\bar{g}_K a_i (V - E_K)$, the steady-state current through a single channel in state i, occur (we assume) on a 10 μs time scale (1). We therefore treat this current, in the millisecond region, as a constant averaged quantity. The term "open-close" kinetics or noise with reference to a K^+ channel has to be understood here in a generalized sense since the channel may be "open" in all states, but to varying degrees. A special case of this sort was considered in reference 1 (Appendix III and Eq. 21). Of course, observed properties of voltage clamp $\bar{I}_K(t)$ curves, such as induction, repolarization decay, superposition (in squid), and linear instantaneous current (in squid), impose severe restraints on possible choices of the α_{ij} and a_i. We shall return to this subject later.

In other examples, a_i would be proportional to optical density in state i, force exerted in state i, etc., depending on the nature of the system and on the actual (fluctuating) quantity being measured.

We come back now to the task of finding the $G(f)$ associated with fluctuations in

N^e. This problem has been considered in a quite formal way by Lax (5) (Eq. 3.12). We first calculate the correlation function as in Eqs. 5, 6, and 38 of reference 1:

$$\begin{aligned} C(t) &= \langle [N(0) - \bar{N}^e] \cdot [N(t) - \bar{N}^e] \rangle \\ &= \langle [N(0) - \bar{N}^e] \cdot [\bar{N}(t; \{N_k(0)\}) - \bar{N}^e] \rangle. \end{aligned} \tag{3}$$

Then $G(f)$ follows from

$$G(f) = 4 \int_0^\infty C(t) \cos 2\pi f t \, dt. \tag{4}$$

From Eqs. 1 and 3,

$$C(t) = \sum_{i,j=0}^{x} a_i a_j \langle [N_i(0) - \bar{N}_i^e] \cdot [\bar{N}_j(t; \{N_k(0)\}) - \bar{N}_j^e] \rangle. \tag{5}$$

To proceed, we need $\bar{N}_j(t)$. As is well known (9), the governing differential equations, in matrix form, are

$$dp/dt = Ap(t), \tag{6}$$

with the formal solution, when A is independent of t,

$$p(t) = \Phi(t) p^0, \Phi(t) \equiv \exp(At). \tag{7}$$

The elements of A are constructed from the α_{ij} in an obvious way (6, 9). Then we can write, in Eq. 5,

$$\bar{N}_j(t) = \sum_{k=0}^{x} \phi_{jk}(t) N_k(0), \tag{8}$$

and (a special case)

$$\bar{N}_j^e = \sum_{k=0}^{x} \phi_{jk}(t) \bar{N}_k^e, \tag{9}$$

where the ϕ_{jk} are the elements of Φ. With these substitutions and use of the variances (6)

$$\begin{aligned} \sigma_{ij}^2 &= -M p_i^e p_j^e \quad (i \neq j), \\ &= M p_i^e (1 - p_i^e) \quad (i = j), \end{aligned} \tag{10}$$

Eq. 5 becomes

$$C(t) = M \sum_{i,j=0}^{x} a_i a_j \phi_{ij}(t) p_j^e - M \sum_{i,j=0}^{x} a_i a_j p_i^e p_j^e. \tag{11}$$

In general, the $\phi_{ij}(t)$ can be expressed as

$$\phi_{ij}(t) = \sum_{k=0}^{x} \gamma_{ij}^{k} e^{\lambda_k t}, \tag{12}$$

where the λ_k are the eigenvalues of A. We limit ourselves here to the case in which these are distinct and negative except for one ($\lambda_0 ; k = 0$) which is zero ($\lambda_0 = 0$). (Actually, this is not a limitation for equilibrium systems.) Thus $\phi_{ij}(\infty) = \gamma_{ij}^{0}$. From Eq. 7, we also have

$$p_i^e = \sum_{j=0}^{x} \phi_{ij}(\infty) p_j^0 . \tag{13}$$

Since the set p_j^0 is completely arbitrary (except for normalization), we can take, say $p_l^0 = 1$ ($p_j^0 = 0, j \neq l$) and find

$$\phi_{ij}(\infty) = \gamma_{ij}^{0} = p_i^e . \tag{14}$$

If we now substitute Eqs. 12 and 14 in Eq. 11, the $k = 0$ terms in the first sum in Eq. 11 cancel the second sum. Hence,

$$C(t) = M \sum_{k=1}^{x} g_k e^{\lambda_k t}, \tag{15}$$

where

$$g_k = \sum_{i,j=0}^{x} a_i a_j \gamma_{ij}^{k} p_j^e . \tag{16}$$

Then, from Eq. 4,

$$G(\omega) = 4M \sum_{k=1}^{x} \frac{-\lambda_k g_k}{\lambda_k^2 + \omega^2}, \tag{17}$$

where $\omega = 2\pi f$.

The total fluctuation (all frequencies) in N^e can be written in various ways:

$$\int_0^\infty G(f)\, df = M \sum_{k=1}^{x} g_k = C(0), \tag{18}$$

$$= \sum_{i,j=0}^{x} a_i a_j \sigma_{ij}^2 , \tag{19}$$

$$= M\left[\sum_{i=0}^{x} a_i^2 p_i^e - \left(\sum_{i=0}^{x} a_i p_i^e\right)^2\right], \tag{20}$$

$$= M[\overline{a^2} - (\bar{a})^2]. \tag{21}$$

In this notation, $\bar{N}^e = M\bar{a}$. To verify that Eqs. 11 and 20 are consistent, we can use the same kind of argument as employed in Eqs. 13 and 14 to show that

$$\phi_{ij}(0) = \delta_{ij}. \tag{22}$$

At low frequencies, G is a constant, $G(0)$:

$$G(0) = 4M \sum_{k=1}^{x} g_k/(-\lambda_k). \tag{23}$$

At high frequencies, $G \sim 1/\omega^2$:

$$\lim_{\omega\to\infty} G(\omega) = (4M/\omega^2) \sum_{k=1}^{x} (-\lambda_k g_k). \tag{24}$$

The "corner" frequency f_c or $\omega_c = 2\pi f_c$ is defined as the frequency at which these two curves (both are straight lines in a log G vs. log ω plot) intersect:

$$\omega_c^2 = \left[\sum_{k=1}^{x} (-\lambda_k g_k)\right] \Big/ \sum_{k=1}^{x} g_k/(-\lambda_k). \tag{25}$$

Equilibrium at $t = \infty$

In order to be able to use the methods and results in reference 9 (p. 24–26), we now specialize to the equilibrium case. Systems with cooperativity are not excluded. That is, there is detailed balance at $t = \infty$:

$$\alpha_{ij}p_i^e = \alpha_{ji}p_j^e. \tag{26}$$

Incidentally, this is not a limitation in the K^+ noise case because we assume that, at steady state, K^+ channels are at equilibrium though the ion transport *through* a channel is a steady-state (nonequilibrium) phenomenon. This assumption is made implicitly or explicitly in the earlier papers of this series and in HH (2).

Our object is to find a useful explicit expression for γ_{ij}^k in Eq. 16. We begin by defining (9) the matrix S by

$$S = B^{-1}AB \tag{27}$$

where the elements of B and B^{-1} are

$$b_{ij} = (p_i^e)^{1/2}\delta_{ij}, \qquad b_{ij}^{-1} = (p_i^e)^{-1/2}\delta_{ij}. \tag{28}$$

Because of detailed balance, S is a real, symmetric matrix. Its eigenvalues are the λ_k (distinct and negative, except for $\lambda_0 = 0$), the same as those of A. Because S is real and symmetric, its eigenfunctions are orthogonal. We next define a matrix U whose

columns are the orthonormal eigenfunctions of S. Hence U is an orthogonal matrix and $U = U^{-1}$ (U is the transpose of U). (In general, U is not symmetric.) It then follows that (10)

$$U^{-1}SU = D(\lambda_i), \tag{29}$$

and

$$U^{-1}B^{-1}ABU = D(\lambda_i), \tag{30}$$

where D is a diagonal matrix with diagonal elements λ_i. Also,

$$\begin{aligned} U^{-1}B^{-1}A &= D(\lambda_i)U^{-1}B^{-1} \\ U^{-1}B^{-1}A^l &= [D(\lambda_i)]^l U^{-1}B^{-1} = D(\lambda_i^l)U^{-1}B^{-1}. \end{aligned} \tag{31}$$

From Eq. 7,

$$\Phi(t) = \exp(At) = \sum_{l=0}^{\infty} \frac{1}{l!} A^l t^l,$$

and hence, using Eq. 31,

$$U^{-1}B^{-1}\Phi(t) = \sum_{l=0}^{\infty} \frac{t^l}{l!} D(\lambda_i^l)U^{-1}B^{-1}$$

$$BUU^{-1}B^{-1}\Phi(t) = \Phi(t) = \sum_{l=0}^{\infty} \frac{t^l}{l!} BUD(\lambda_i^l)U^{-1}B^{-1},$$

or

$$\Phi(t) = BUD(e^{\lambda_i t})U^{-1}B^{-1}. \tag{32}$$

Using $U^{-1} = U$, we find for the elements of Φ,

$$\phi_{ij}(t) = (p_i^e)^{1/2}(p_j^e)^{-1/2} \sum_{k=0}^{x} u_{ik}u_{jk}e^{\lambda_k t}, \tag{33}$$

and therefore, from Eq. 12,

$$\gamma_{ij}^k = (p_i^e)^{1/2}(p_j^e)^{-1/2}u_{ik}u_{jk}. \tag{34}$$

Thus, the γ_{ij}^k may be obtained easily from the eigenfunctions of S.

Incidentally, Eqs. 14 and 34 give

$$u_{i0} = (p_i^e)^{1/2}. \tag{35}$$

Also, from Eqs. 22 and 33, we have

$$\sum_{k=0}^{x} u_{ik}u_{jk} = \delta_{ij}. \tag{36}$$

Thus, the rows of U (as well as the columns) form a set of orthonormal vectors. This can be shown directly from $\tilde{U} = U^{-1}$.

Substitution of Eq. 34 in Eq. 16 leads to

$$g_k = \left[\sum_{i=0}^{x} a_i (p_i^e)^{1/2} u_{ik}\right]^2. \tag{37}$$

This can now be used in Eqs. 15–25.

If the ensemble starts at $t = 0$ in the arbitrary state p^0, the time dependence of $\bar{N}$ follows from Eqs. 1, 8, and 25:

$$\bar{N}(t) = M \sum_{k=0}^{x} q_k e^{\lambda_k t}, \tag{38}$$

where

$$q_k = \left[\sum_{i=0}^{x} a_i (p_i^e)^{1/2} u_{ik}\right]\left[\sum_{j=0}^{x} p_j^0 (p_j^e)^{-1/2} u_{jk}\right]. \tag{39}$$

At $t = \infty$, we have

$$\bar{N}^e/M = q_0 = g_0^{1/2} = \sum_{i=0}^{x} a_i p_i^e = \bar{a}. \tag{40}$$

For an arbitrary kinetic scheme (leading to equilibrium at $t = \infty$), the eigenvalues and eigenfunctions of S can be calculated by matrix manipulations if x is small, say $x = 2$ or 3. With a larger number of states, say with $x \leqslant 50$, the problem can still be handled numerically by computer.

We turn next to the case of particular interest here. Because of its unusual simplicity, analytical expressions may be found for the g_k and q_k.

System Composed of x Independent and Equivalent Subunits

In this special case (essentially HH) each subunit has two possible states or conformations with the kinetic scheme.

$$(i) \underset{\beta}{\overset{\alpha}{\rightleftarrows}} (ii). \tag{41}$$

Multistate subunit models (11) are, of course, also possible, but will not be considered here. The probability of subunit state ii is n and of subunit state i is $1 - n$.

The kinetic scheme for a system of x subunits is then (as in Eq. 29 of reference 1)

$$[0] \underset{\beta}{\overset{x\alpha}{\rightleftarrows}} [1] \underset{2\beta}{\overset{(x-1)\alpha}{\rightleftarrows}} \cdots \underset{x\beta}{\overset{\alpha}{\rightleftarrows}} [x].$$

$$(p_0) \qquad (p_1) \qquad\qquad (p_x) \tag{42}$$

The system state $[j]$ with probability p_j has j subunits in state ii. This scheme is not only sequential (transitions limited to $j \to j+1$ and $j \to j-1$) but also the α_{ij} are very simple. Eq. 42 would also apply to other two-state subunit models, e.g. Langmuir adsorption on a system of x sites (8). Symbolically, Eq. 42 is the same as $[(i) \rightleftarrows (ii)]^x$.

We restrict ourselves here to initial states ($t = 0$) in which the ensemble is in equilibrium. This does not affect the noise calculation (at $t = \infty$), but, of course, does influence the kinetics. Initial equilibrium obtains in the usual voltage clamp ("V jump") experiment in the K^+ current case.

We write $n = n_0$ at $t = 0$ and $n = n_\infty$ at $t = \infty$. Then (as in Eq. 34 of reference 1)

$$p_i(t) = \frac{x!n(t)^i[1 - n(t)]^{x-i}}{i!(x-i)!}, \tag{43}$$

where

$$n(t) = n_\infty + (n_0 - n_\infty)e^{-t/\tau}$$
$$n_\infty = \alpha/(\alpha + \beta), \qquad \tau = 1/(\alpha + \beta). \tag{44}$$

In the K^+ current application, α, β, n_∞, and τ are all functions of the parameter V.

In our previous work (1) we found $C(t)$ and $G(\omega)$ in the HH case, $a_0 = a_1 = \cdots = a_{x-1} = 0$, and in the "$\kappa$ case," $a_{x-1} = \kappa < 1$, $a_{x-2} = \kappa^2$, $\cdots$, $a_0 = \kappa^x$ (conductance reduced by a factor κ for each subunit in state i). In the present paper, the kinetic scheme (HH) is the same as in reference 1 but the a_i's are arbitrary.

Quite aside from information that may be forthcoming from future noise measurements, well-known properties of $\bar{I}_K(t)$ in voltage clamp experiments put considerable limitations on the a_i's. For example, if the a_i's are functions of V with "instantaneous" relaxation on a millisecond time scale (as is the case with α and β), then the observed (2, 12) approximate linear instantaneous K^+ current (squid) would not be found. If the $a_i(V)$ relax on a millisecond scale, the observed approximate superposition (13) of $\bar{I}_K(t)$ curves (squid) would be lost. But any constant set of a_i's (with Eq. 42) provides superposition and a linear instantaneous current. Thus for squid at least, the a_i's must be substantially independent of V—which is what would be expected if the origin of $a_i < 1$ ($i < x$) is steric hindrance of K^+ ions owing to subunits in the "wrong" conformation, i. One can say further that the "early" a_i's (a_0, a_1, $\cdots$) must be zero or relatively small in order to provide the observed

induction behavior in $I_K(t)$ near $t = 0$ in depolarizations from the neighborhood of the rest potential. Full-scale curve fitting (including repolarizations) would, of course, provide further information about the a_i's. As a footnote, it should be mentioned that an arbitrary equilibrium kinetic scheme, as in the preceding subsection, even a sequential one with constant a_i's, will in general not provide superposition. This subject has been discussed elsewhere (14, 15).

We turn now to the necessary mathematics. It is obvious from Eqs. 43 and 44 that in this case the eigenvalues λ_k must be

$$\lambda_k = -k/\tau \qquad (k = 0, 1, \cdots, x). \tag{45}$$

The matrix U (columns of U = orthonormal eigenfunctions of S) is given in the Appendix for $x = 2, 3, 4$. U is symmetric in this special case. The p_i^e and p_i^0 are provided by Eq. 43 with $n = n_\infty$ and $n = n_0$, respectively. We can then write out g_k and q_k, from Eq. 37 and 39, for $x = 2, 3, 4$. These turn out to be combinations of binomial forms which can easily be generalized to arbitrary x:

$$g_k = \frac{x![n_\infty(1 - n_\infty)]^k\{\ \}_k^2}{k!(x-k)!}, \tag{46}$$

$$q_k = \frac{x!(n_\infty - n_0)^k\{\ \}_k}{k!(x-k)!}, \tag{47}$$

where

$$\{\ \}_k = \sum_{j=0}^{x-k} \frac{(x-k)!(-n_\infty)^{x-k-j}H_{x-j}}{j!(x-k-j)!}, \tag{48}$$

and

$$H_{x-j} = \sum_{l=0}^{x-j} \frac{(x-j)!(-1)^l a_l}{l!(x-j-l)!}. \tag{49}$$

Eqs. 17 and 46 reduce properly to Eqs. 15 and 21 of reference 1 in the HH and κ cases mentioned above. (Note: the second $e^{-t/\tau}$ in Eq. 20 of reference 1 should be omitted.) Another easy check is the case $a_i = i/x$ (equal increments of conductance for each step $i \rightarrow i + 1$). This is essentially equivalent to HH with $x = 1$, since each subunit in state ii (irrespective of the system state i) makes an equal and independent contribution to $\bar{N}^e$. As a check on Eq. 47, we can successively pick out the coefficients of $a_0, a_1 \cdots$ in Eq. 38 and verify that these coefficients are $Mp_0(t)$, $Mp_1(t)$, $\cdots$, respectively, as given by Eq. 43.

Since $\lambda_k = -k/\tau$, Eqs. 17, 23, and 25 become

$$G(\omega) = 4M\tau \sum_{k=1}^{x} \frac{g_k k}{k^2 + \omega^2\tau^2}, \tag{50}$$

$$G(0) = 4M\tau \sum_{k=1}^{x} (g_k/k), \tag{51}$$

and

$$\omega_c^2 = (1/\tau^2)\left(\sum_{k=1}^{x} g_k k\right) \Big/ \left(\sum_{k=1}^{x} g_k/k\right). \tag{52}$$

When $x = 1$, we have the simple properties

$$G(\omega) = \frac{4M\tau n_\infty (1 - n_\infty)(a_1 - a_0)^2}{1 + \omega^2\tau^2} \tag{53}$$

$$\omega_c = 1/\tau. \tag{54}$$

In the κ case,

$$g_k = \frac{x!\, n_\infty^k (1 - n_\infty)^k (1 - \kappa)^{2k} N_\infty^{2(x-k)}}{k!(x - k)!} \tag{55}$$

where $N_\infty = n_\infty + \kappa(1 - n_\infty)$. In the HH case ($\kappa = 0$),

$$g_k = \frac{x!\, n_\infty^{2x-k}(1 - n_\infty)^k}{k!(x - k)!}. \tag{56}$$

From Eq. 21 of reference 1 (or Eq. 52), in the κ case,

$$\omega_c^2 = (1/\tau^2)(N_\infty + A)^{x-1} \Big/ \sum_{k=1}^{x} \frac{(x - 1)!\, N_\infty^{x-k} A^{k-1}}{(k - 1)!(x - k)!k^2}, \tag{57}$$

where

$$A = n_\infty(1 - \kappa)(1 - N_\infty)/N_\infty. \tag{58}$$

In the HH case,

$$\omega_c^2 = (1/\tau^2) \Big/ \sum_{k=1}^{x} \frac{(x - 1)!\, n_\infty^{x-k}(1 - n_\infty)^{k-1}}{(k - 1)!(x - k)!\, k^2}. \tag{59}$$

In Eqs. 55–59, κ is constant but τ and n_∞ are functions of V.

As we shall see in the next two sections, there is some interest (3) in ω_c in the limits $V \to +\infty$ and $V \to -\infty$ where $n_\infty \to 1$ and $n_\infty \to 0$, respectively. In the HH case, we find (3)

$$\omega_c \to x/\tau(V) \quad \text{when } n_\infty \to 0$$

$$\omega_c \to 1/\tau(V) \quad \text{when } n_\infty \to 1. \tag{60}$$

In the κ case,

$$\omega_c \to 1/\tau(V) \quad \text{when } n_\infty \to 0 \text{ or } n_\infty \to 1. \tag{61}$$

In the more general model (arbitrary a_i's), careful examination of Eq. 52 when $n_\infty \to 0$ shows that, if $H_1 = H_2 = \cdots = H_{\alpha-1} = 0$ but $H_\alpha \neq 0$, where $1 \leqslant \alpha \leqslant x$, then $\omega_c \to \alpha/\tau$ in this limit. According to Eq. 49, this condition on the H's is the same as $a_0 = a_1 = \cdots = a_{\alpha-1}$, but $a_\alpha \neq a_{\alpha-1}$. In the HH case, $\alpha = x$; in the κ case, $\alpha = 1$. Indeed, *any* model with $a_0 \neq a_1$ will give $\omega_c \to 1/\tau$ when $n_\infty \to 0$. Because of the symmetry of the model, analogous comments apply when $n_\infty \to 1$, but with the order of the a_i's reversed. For example, in this latter limit, $\omega_c \to 1/\tau$ whenever $a_x \neq a_{x-1}$ (in agreement with Eqs. 60 and 61).

3. DISCUSSION

Before presenting sample calculations in the next section, we first make some necessary related comments on the papers by Lax (5), Stevens (4), and Fishman (3).

Range of Validity of the Theory

We follow Lax (5), who has discussed the matter in detail, in assuming with confidence that the method of calculation of the noise spectrum used in section 2 is valid for a linear system at equilibrium or steady state (as explained above, our primary interest here is in the equilibrium case). By "linear," we mean that the state variables p whose fluctuations are being studied follow kinetic equations of the form $\mathrm{d}p/\mathrm{d}t \sim p$, as in Eq. 6. (Lax calls this "quasilinear.") If there are x independent variables of this sort, there will be x terms (and x time constants) in $C(t)$ (Eq. 15) and x terms in $G(\omega)$ (Eq. 17).

The regime of irreversible thermodynamics, very near equilibrium, is much more limited than this. In this regime we have not only $\mathrm{d}p/\mathrm{d}t \sim p$ but also the more restrictive $p - p^e \sim X$ (thermodynamic forces). (Lax refers to this as "complete linearity.") Correspondingly, if one made a noise calculation in the "very near equilibrium" *approximation*, one would use $C(t) \sim e^{\lambda_1 t}$ (λ_1 is the eigenvalue nearest zero) and find $G(\omega) \sim (\lambda_1^2 + \omega^2)^{-1}$ (one term). But, in general ($x > 1$), this would be both a bad and unnecessary approximation. On the other hand, these one-term expressions for $C(t)$ and $G(\omega)$ would be exact for any linear system with only one independent state variable ($x = 1$), provided that this is also the "noise" variable of interest.

Stevens (4) independently derived Eqs. 14 and 15 of reference 1 for $C(t)$ and $G(\omega)$ in the HH case with $x = 4$. Among a number of other topics, he also considered (as a K^+ channel model) noise in the quantity n^4, where n is a "continuous" variable which follows the usual HH linear kinetics (see Eq. 41 and 44). This is a single state variable problem but we require the noise spectrum of a nonlinear

function (n^4) of this variable. To bring this model within the scope of the class of linear systems above, we linearize, following Stevens (4):

$$\nu \equiv n - n_\infty, \Delta \equiv n^4 - n_\infty^4,$$

$$d\nu/dt = -\nu/\tau, n^4 = n_\infty^4 + 4n_\infty^3 \nu + 0(\nu^2),$$

$$\Delta \cong 4n_\infty^3 \nu, d\Delta/dt \cong -\Delta/\tau. \quad (62)$$

The last (approximate) equation has the required linear form and leads immediately to

$$C(t) \sim e^{-t/\tau}, G(\omega) \sim (1 + \omega^2\tau^2)^{-1}. \quad (63)$$

But it must be emphasized that this simple one-term $G(\omega)$ is *not* the true noise spectrum of the quantity n^4 but only an approximation to it; linearization is used for a good and proper reason, but it is an approximation all the same.

Examples of nonlinear noise calculations are given by Lax (5) and van Kampen (16). One-term $G(\omega)$'s are not found.

Incidentally, quite aside from the above mathematical considerations, we find it difficult to visualize, at the required molecular level, a continuous (4) (rather than probabilistic) variable n which would follow kinetics of the form $dn/dt = \alpha(1 - n) - \beta n$ and which would determine a channel conductance proportional to n^4.

Relation to the Fishman (3) *Paper*

We have emphasized the status of various one-term $G(\omega)$'s above because Fishman's (3) preliminary corner frequency results seem compatible with a one-term $G(\omega)$. Any one-term $G(\omega)$ gives, for the V dependence of ω_c, $\omega_c = 1/\tau(V)$ where τ is the single time constant. Fishman compares his experimental points of $f_c(V)$ with a plot (solid curve, his Fig. 2 *a*) of $f_c(V) = 1/[2\pi\tau(V)]$, where $\tau(V)$ is taken as the original HH $\tau_n(V)$ function (2). The agreement between the solid curve and the somewhat scattered experimental points is fairly good. We have several comments to make on this subject:

(*a*) As emphasized by Fishman, the data and data analysis need refinement, and $\tau(V)$ should be obtained (by an HH type of $I_K(t)$ analysis) from the same noise axons rather than from the HH axons (2). Hence the agreement referred to above could be somewhat fortuitous.

(*b*) As a matter of fact, $\tau(V)$ in $f_c = 1/[2\pi\tau(V)]$ should be found by fitting $I_K(t)$ data not with the HH formalism but with the same theoretical model which produces $G(\omega) \sim (1 + \omega^2\tau^2)^{-1}$ and $f_c = 1/[2\pi\tau(V)]$. The only models that give a true one-term $G(\omega)$ are those in which the K^+ conductance is proportional to a single-state variable and this variable obeys linear kinetics (e.g. HH with $x = 1$). But

$I_K(t)$ has a simple exponential form (Eq. 44) for such models and will not fit experimental $I_K(t)$ curves (e.g. early induction behavior in depolarizations requires $x \geq 3$ in HH). In this connection, we note that the one-term $G(\omega)$ in Eq. 63 for the "continuous n" version of HH is excluded here because it is not the true $G(\omega)$ for the model.

The HH $\tau(V)$ for $x = 4$ (whether from HH [2] or from the noise axons) should only be used in the appropriate HH ω_c expression, namely, Eq. 59 with $x = 4$. The HH $n_\infty(V)$ for $x = 4$ is also needed in this equation. The dashed curve in Fishman's Fig. 2 *a* was obtained in this way [using the original HH $\tau_n(V)$ and $n_\infty(V)$]. Despite the uncertainties mentioned under *a* above, Fishman (3) believes that the discrepancy between the dashed curve and his experimental points makes the original HH model ($a_0 = a_1 = \cdots = a_{x-1} = 0$ in our notation) unlikely.

A final comment: Fishman labels his solid curve, $f_c = 1/[2\pi\tau(V)]$, "multistate." This seems a misnomer since it can arise only from a two-state ([0] and [1]; $x = 1$) model, or the kinetic equivalent. Actually, as far as a noise calculation is concerned, the HH $x = 4$ case (dashed curve) is a multistate one (Eq. 42). That is, all states [0], $\cdots$, [4] have to be considered in the analysis even though the channel is open only in state [4]. We are referring here to channel (or system) states. To avoid confusion in multisubunit models, one must distinguish between subunit states and channel (system) states, as is done in Eqs. 41 and 42.

(*c*) Theoretical curves of $f_c(V)$, similar to but not the same as $1/[2\pi\tau(V)]$, follow from the multistate (channel) κ model and from variations on the κ model (section 4). These models can fit the kinetic data (see Appendix III of reference 1), including induction, repolarization decay, superposition, and linear instantaneous current, and in some cases they also fit the available experimental $f_c(V)$ data as well as or better than the HH $1/[2\pi\tau(V)]$. Hence, they appear to be "the most likely [present] possibility" (3). It should be emphasized that this class of models is still of the basic HH type (Eqs. 41 and 42); they differ from the original HH model only in the choice of a_i's (the channel conducts somewhat in states other than $i = x$).

Some examples of the theoretical $f_c(V)$ curves just mentioned are included in the next section.

4. SAMPLE CALCULATIONS

Though the equations in this paper cover a rather broad class of K^+ channel models it would be inappropriate to publish extensive theoretical calculations at this time because of the necessarily preliminary nature of the only experiments available for guidance (3). Our main object in this section will therefore be to show that a few rather arbitrary choices of a_i's give $f_c(V)$ curves which fit Fishman's corner frequency data more or less as well as the function $1/[2\pi\tau(V)]$ used by Fishman. As already explained the latter function is inappropriate in the present application for various reasons. We merely want to make it clear here that many models exist which

are free from the objections we have raised concerning $1/[2\pi\tau(V)]$. Furthermore, these models are basically of the HH type (Eqs. 41 and 42).

We shall also include examples of $G^T \equiv C(0)$ (T is the total fluctuation, Eq. 18) and the low frequency plateau of the noise spectrum $G^0 \equiv G(0)$ (Eq. 23). These functions might supplement $f_c(V)$ as diagnostic aids in model testing. Some other properties of $G(\omega)$ could also be used. Incidentally, comparison of Eq. 2 with Eqs. 3 and 18 of reference 1 makes it clear that the actual power spectrum in the K^+ current, $G_I(\omega)$, is related to $G(\omega)$, as in reference 1, by

$$G_I(\omega) = G(\omega) \cdot g_K^2(V - E_K)^2. \tag{64}$$

The V-dependent factor $g_K^2(V - E_K)^2$ does not affect $f_c(V)$ but it would multiply both $G^T(V)$ and $G^0(V)$ to give $G_I^T(V)$ and $G_I^0(V)$. For simplicity, we use $G^T(V)$ and $G^0(V)$ in Figs. 3 and 4 below [corresponding to experimental values divided by $g_K^2(V - E_K)^2$].

Our calculations here will be based on the original HH data. Ideally, for a given set of constant a_i's, that is, for a given choice of a model within the HH class (Eqs. 41 and 42), we would determine $\tau(V)$ and $n_\infty(V)$ by fitting the HH voltage clamp K^+ conductance data with Eqs. 38, 45, and 47. However, such a detailed procedure is unwarranted in these sample calculations. Instead, we shall let the HH empirical functions $\tau(V)$ and $n_\infty(V)$ represent their data and use a relatively simple argument to deduce modified or "corrected" $\tau(V)$ and $n_\infty(V)$ functions for *each* different a_i set used in our calculations. To avoid confusion, in the following we designate the original HH functions (for $x = 4$) by $\tau^H(V)$ and $n_\infty^H(V)$.

We employ the same V scale as Fishman: $V = 0$ at the rest potential; $V > 0$ for depolarizations therefrom. The procedure used to obtain $\tau(V)$ and $n_\infty(V)$, for each a_i set, is the following. To find $n_\infty(V)$, we first note from Eqs. 40 and 47 that

$$\frac{\bar{N}^e}{M} = q_0 = \{\ \}_0 = \sum_{j=0}^{x} \frac{x!(-n_\infty)^{x-j} H_{x-j}}{j!(x-j)!}. \tag{65}$$

The range of n_∞ is $0 \leqslant n_\infty \leqslant 1$ (Eq. 44) and of $\bar{N}^e/M$ is $a_0 \leqslant \bar{N}^e/M \leqslant 1$ (since $a_x = 1$). The quantity $\bar{N}^e/M$ corresponds to $[n_\infty^H(V)]^4$ in the HH formulation (see Eq. 2). Thus, for each V, $[\ ]^4$ from HH gives us the value of $q_0(V)$, from which we can then find $n_\infty(V)$ (using Eq. 65). Note that $n_\infty = 1$ when $n_\infty^H = 1$. Also, $n_\infty = 0$ when $n_\infty^H = 0$ if and only if we select $a_0 = 0$ (as we do below). With $a_0 = 0$, the K^+ conductance $g_K \to 0$ as $V \to -\infty$ (as in HH). In the κ case, on the other hand, when $n_\infty \to 0$ we have $\bar{N}^e/M \to a_0 = \kappa^x$ (but this would usually be a very small quantity).

A simple (but certainly not unique) way to find $\tau(V)$ for the given a_i set is to match $t_{1/2}$ values (in hypothetical depolarizations or repolarizations) in the a_i case with those from the HH functions ($x = 4$), where $t_{1/2}$ is an appropriate half-

time. Because we are especially interested in values of V on both sides of $V = 0$ (rest potential), we use repolarizations to an arbitrary V starting from $V = +\infty$ (where $n_\infty^H = n_\infty = 1$). At $t = 0$, in such repolarizations, $q_0 = [\ ]^4 = 1$. At $t = \infty$ $q_0(V) = [n_\infty^H(V)]^4$. Thus we define $t_{1/2}(V)$ by the equation

$$[n^H(t_{1/2})]^4 = \frac{1 + [n_\infty^H(V)]^4}{2}. \tag{66}$$

From Eq. 44 with $n_o = 1$, it is easy to derive an expression for, and to calculate, $t_{1/2}(V)$ as a function of $n_\infty^H(V)$ and $\tau^H(V)$. For each V, we then employ (Eq. 38)

$$\frac{1 + [n_\infty^H(V)]^4}{2} = \sum_{k=0}^{x} q_k\, e^{-kt_{1/2}(V)/\tau} \tag{67}$$

to find $\tau(V)$. In q_k here, we put $n_o = 1$ (Eq. 47) and use $n_\infty(V)$ as already determined from Eq. 65.

With $\tau(V)$ and $n_\infty(V)$ available, we can now turn to calculations based on Eqs. 18, 46, 51, and 52. In Figs. 1 *a*, *b*, and *c* we plot ω_c as a function of V in "modified κ cases." These are "κ cases" except that we take $a_0 = 0$ rather than $a_0 = \kappa^x$ (see above). Actually, with the small values of κ used, the difference is a matter of convenience only. These three figures are for $x = 3$, 4, and 6, respectively. For a more detailed consideration of different x values, see reference 1. The dashed curve labeled $1/\tau^H(V)$ (for $x = 4$ in all figures) is included for reference purposes because Fishman's experimental points scatter more or less around this curve (3), though the points tend to be above the curve in the neighborhood of $V = 0$. The top curve in each of these figures is for $\kappa = 0$ (i.e., for HH with $x = 3$, 4, 6; Eq. 59). On this scale these $\kappa = 0$ curves are virtually independent of x (compare Fig. 1 of reference 1). The asymptotic properties for $\kappa = 0$ are given by Eq. 60. The other solid curves in each figure are for $\kappa > 0$. As anticipated in Eqs. 60 and 61, and in the discussion following these equations, there is a considerable difference between the $\kappa = 0$ (HH) and the $\kappa > 0$ cases when $V < 0$. Some of the $\kappa > 0$ curves seem to follow Fishman's experimental points better than does $1/\tau^H(V)$ (as already discussed in section 3).

We emphasize again that each solid curve in Figs. 1 *a*, *b*, and *c* has its own $\tau(V)$ and $n_\infty(V)$. As an illustration of this, the $1/\tau(V)$ curve (dotted) for $x = 3$, $\kappa = 0.05$ is included in Fig. 1 *a*. It determines the asymptotic behavior of $\omega_c(V)$ at $V \to \pm\infty$, and it illustrates the "correction" of $\tau^H(V)$ (bottom curve) to give $\tau(V)$. It should be mentioned that all of our calculations are for 6°C (HH), while Fishman's Fig. 2 *a* has been scaled to 12.5°C (using $Q_{10} = 3$).

Fig. 2, for $x = 4$, illustrates another physically reasonable choice of the a_i's: $a_3 = \kappa$, $a_2 = \kappa/2$, $a_1 = \kappa/3$, $a_0 = 0$. This case was also mentioned in reference 1, except that here again we take $a_0 = 0$ (instead of $a_0 = \kappa/4$) to give $g_k \to 0$ as $V \to -\infty$. The $\kappa = 0$ (HH) curve is the same as in Fig. 1 *b*, and the reference

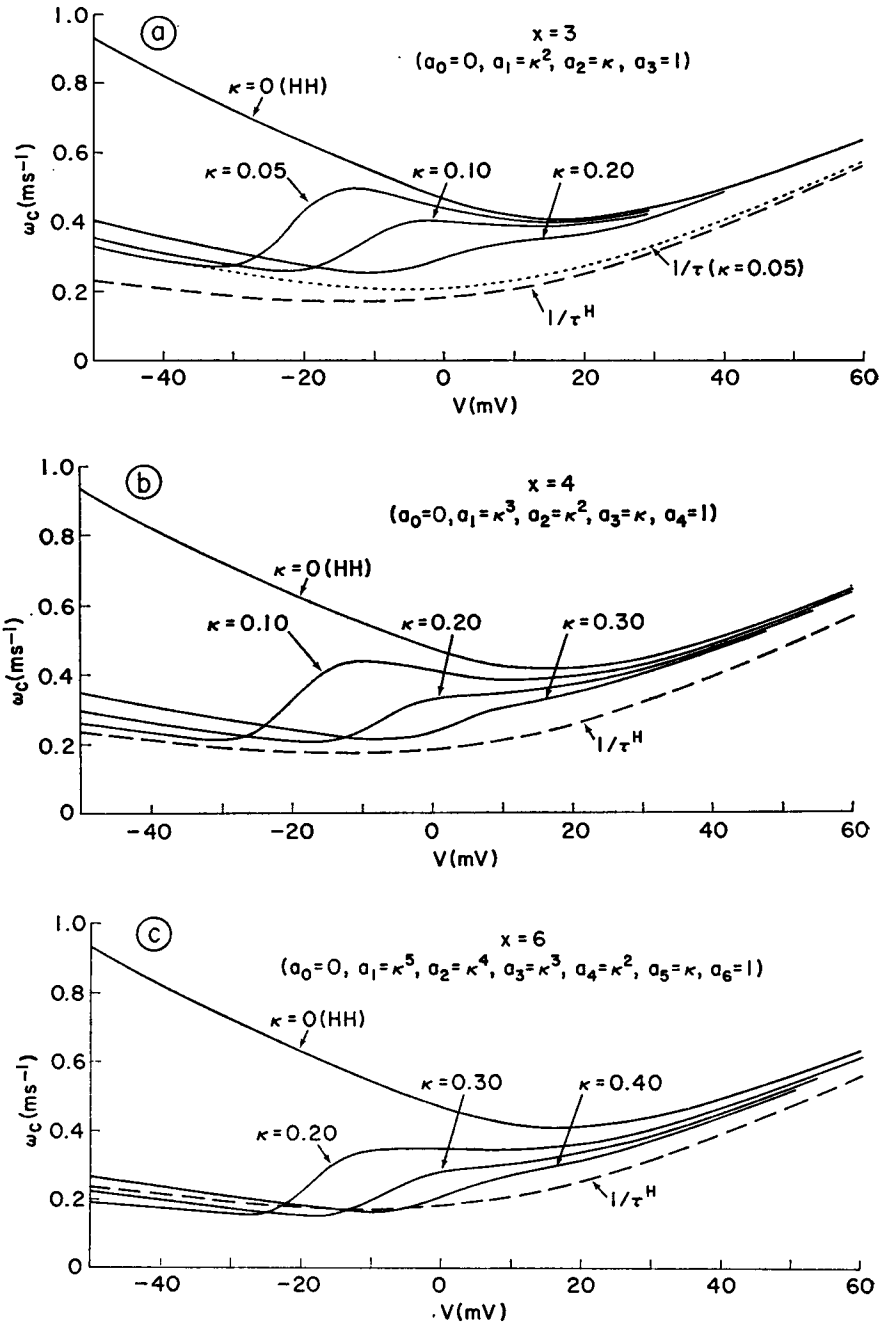

FIGURE 1 Corner frequency $\omega_c = 2\pi f_c$ as a function of V. $V = 0$ at rest potential; $V > 0$ for depolarizations. Modified κ case. $\tau^H = HH\,\tau_n(V)$ for $x = 4$. (*a*) $x = 3$; (*b*) $x = 4$; (*c*) $x = 6$. See text for further details.

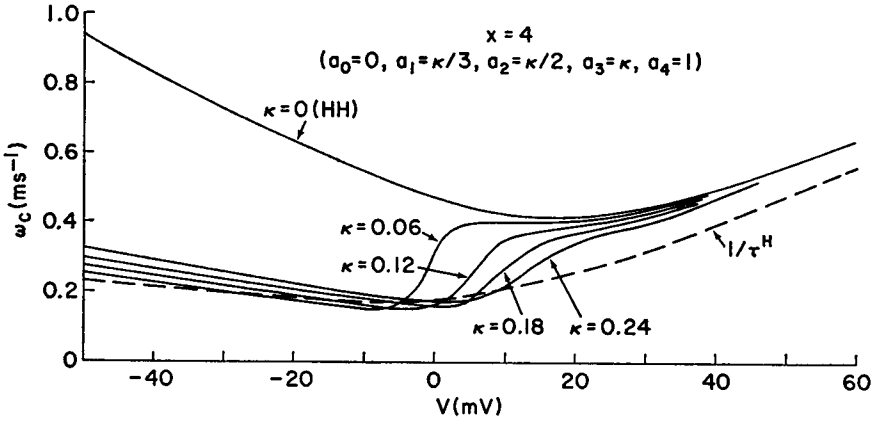

FIGURE 2 Corner frequency $\omega_c = 2\pi f_c$ as a function of V. $V = 0$ at rest potential; $V > 0$ for depolarizations. The a_i values are indicated in the figure; $x = 4$. See text for further details.

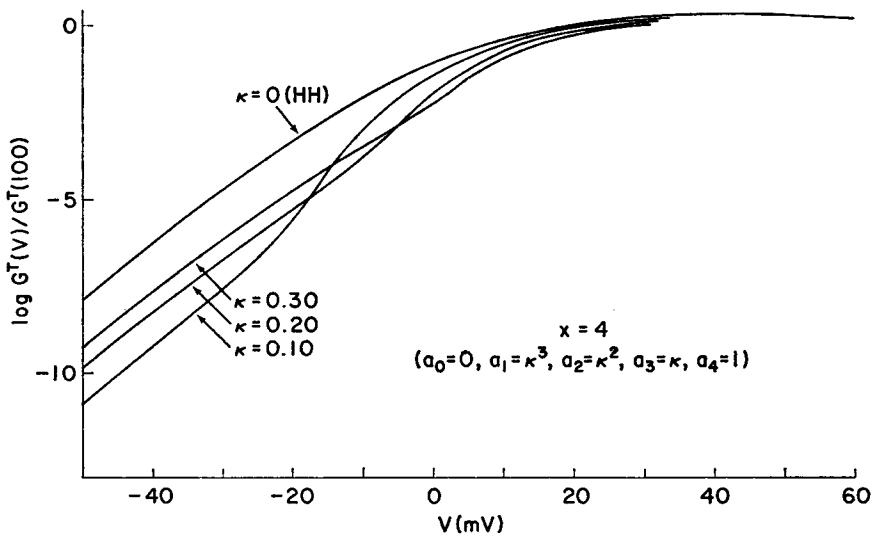

FIGURE 3 Logarithm of total fluctuation $G^T(V) \equiv C(0)$ as a function of V for the same case as in Fig. 1 *b*. G^T at $V = 100$ mV is used as a reference point.

curve $1/\tau^H(V)$ is the same as in Figs. 1 *a*, *b*, and *c*. The "transition" near $V = 0$ is somewhat sharper than in Figs. 1 *a*, *b*, and *c*. No doubt many other choices of a_i's would give similar results, so long as a_0 (small or zero) $\neq a_1$ and $a_{x-1} \neq a_x$ (Eq. 61).

Figs. 3 and 4 show, respectively, families of curves of log $G^T(V)/G^T(100)$ and log $G^0(V)/G^0(100)$ for the $x = 4$ modified κ case. The choice of $V = 100$ m V for the reference value is arbitrary. The two families are quite similar, which is not

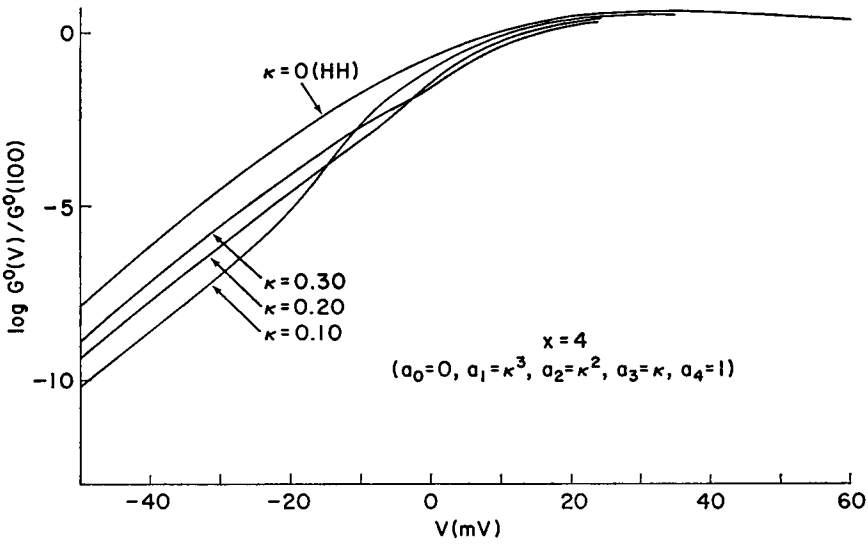

FIGURE 4 Logarithm of low frequency $G^0(V) \equiv G(0)$ as a function of V for the same case as in Fig. 1 *b*. G^0 at 100 mV is used as a reference point.

surprising. Since $G^0(V)$ is much easier to obtain from experimental data than $G^T(V)$, this similarity suggests that $G^0(V)$ may be more useful in model diagnosis than $G^T(V)$.

Finally, a word of caution. Following Fishman (3), we have extended our calculations in Figs. 1–4 to $V = -50$ mV. In doing this, we are assuming that $\tau^H(V)$ and $n_\infty{}^H(V)$ are reliable to $V = -50$ mV. For the latter function, at least, this is a doubtful assumption (2, 11, 13). Figs. 3 and 4, especially, would be affected (for $V < 0$).

APPENDIX

The U matrices for Eq. 42, with $x = 2, 3, 4$, are given below. The eigenvalue associated with each column is indicated. For simplicity in printing, we write n for n_∞ here.

$$x = 2$$

$$\begin{pmatrix} [(1-n)^2]^{1/2} & [2n(1-n)]^{1/2} & [n^2]^{1/2} \\ [2n(1-n)]^{1/2} & [(2n-1)^2]^{1/2} & -[2n(1-n)]^{1/2} \\ [n^2]^{1/2} & -[2n(1-n)]^{1/2} & [(1-n)^2]^{1/2} \\ 0 & -1/\tau & -2/\tau \end{pmatrix}$$

$$x = 3$$

$$\begin{pmatrix} [(1-n)^3]^{1/2} & [3n(1-n)^2]^{1/2} & [3n^2(1-n)]^{1/2} & [n^3]^{1/2} \\ [3n(1-n)^2]^{1/2} & [(3n-1)^2(1-n)]^{1/2} & [(3n-2)^2n]^{1/2} & -[3n^2(1-n)]^{1/2} \\ [3n^2(1-n)]^{1/2} & [(3n-2)^2n]^{1/2} & -[(3n-1)^2(1-n)]^{1/2} & [3n(1-n)^2]^{1/2} \\ [n^3]^{1/2} & -[3n^2(1-n)]^{1/2} & [3n(1-n)^2]^{1/2} & -[(1-n)^3]^{1/2} \\ 0 & -1/\tau & -2/\tau & -3/\tau \end{pmatrix}$$

$$x = 4$$

$$\begin{vmatrix} [(1-n)^4]^{1/2} & [4n(1-n)^3]^{1/2} & [6n^2(1-n)^2]^{1/2} & & \\ & & & [4n^3(1-n)]^{1/2} & [n^4]^{1/2} \\ [4n(1-n)^3]^{1/2} & [(4n-1)^2(1-n)^2]^{1/2} & [6n(1-n)(2n-1)^2]^{1/2} & & \\ & & & [n^2(4n-3)^2]^{1/2} & -[4n^3(1-n)]^{1/2} \\ [6n^2(1-n)^2]^{1/2} & [6n(1-n)(2n-1)^2]^{1/2} & [(6n^2-6n+1)^2]^{1/2} & & \\ & & -[6n(1-n)(2n-1)^2]^{1/2} & [6n^2(1-n)^2]^{1/2} & \\ [4n^3(1-n)]^{1/2} & [(4n-3)^2n^2]^{1/2} & -[6n(1-n)(2n-1)^2]^{1/2} & & \\ & & & [(1-n)^2(4n-1)^2]^{1/2} & -[4n(1-n)^3]^{1/2} \\ & [n^4]^{1/2} & -[4n^3(1-n)]^{1/2} & [6n^2(1-n)^2]^{1/2} & \\ & & & -[4n(1-n)^3]^{1/2} & [(1-n)^4]^{1/2} \\ 0 & -1/\tau & -2/\tau & -3/\tau & -4/\tau \end{vmatrix}$$

We are indebted to Dr. Harvey Fishman for making his manuscript available to us before publication, and also to Dr. Fishman and Dr. Charles Anderson for very helpful discussions.

Received for publication 15 March 1973.

REFERENCES

1. HILL, T. L., and Y. CHEN. 1972. *Biophys. J.* **12**:948. Erratum: **12**; no. 12.
2. HODGKIN, A. L., and A. F. HUXLEY. 1952. *J. Physiol. (Lond.).* **117**:500.
3. FISHMAN, H. M. 1973. *Proc. Natl. Acad. Sci. U.S.A.* **70**:876.
4. STEVENS, C. F. 1972. *Biophys. J.* **12**:1028.
5. LAX, M. 1960. *Rev. Mod Phys.* **32**:25. See also VAN VLIET, K. M. and J. R. FASSETT. 1965. *In* Fluctuation Phenomena in Solids. R. E. Burgess, editor. Academic Press, Inc., New York.
6. HILL, T. L. 1971. *J. Chem. Phys.* **54**:34.
7. KEIZER, J. 1972. *J. Stat. Phys.* **6**:67.
8. HILL, T. L. 1968. Thermodynamics for Chemists and Biologists. Addison-Wesley Publishing Co., Inc., Reading, Mass. Chap. 7.
9. OPPENHEIM, I., K. E. SHULER, and G. H. WEISS. 1967. *Adv. Mol. Relaxation Processes.* **1**:13.
10. MARGENAU, H., and G. M. MURPHY. 1956. The Mathematics of Physics and Chemistry. D. van Nostrand Co., Inc., New York.
11. HILL, T. L., and Y. CHEN. 1972. *Biophys. J.* **12**:960.
12. ADELMAN, W. J., JR., F. M. DYRO, and J. SENFT. 1965. *J. Gen. Physiol.* **48** (5,2):1.
13. COLE, K. S., and J. W. MOORE. 1960. *Biophys. J.* **1**:1.
14. HILL, T. L., and Y. CHEN. 1971. *Proc. Natl. Acad. Sci. U.S.A.* **68**:1711.
15. PAUL, E., and T. L. HILL. 1972. *Proc. Natl. Acad. Sci. U.S.A.* **69**:2246.
16. VAN KAMPEN, N. G. 1965. *In* Fluctuation Phenomena in Solids. R. E. Burgess, editor. Academic Press, Inc., New York.